Journal of the European Ceramic Society **18** (1998) 601–605

PII: S0955-2219(97)00211-2
0955-2219/98/$19.00 + 0.00

Nb– and Cr–Al_2O_3 Composites with Interpenetrating Networks

D. E. García,* S. Schicker, R. Janssen and N. Claussen

Advanced Ceramics Group, TUHH, Technische Universität Hamburg, Harburg 21071, Hamburg, Germany

(Received 22 September 1997; accepted 20 November 1997)

Abstract

Cr–Al_2O_3 and Nb–Al_2O_3 composites containing 50 vol% metal have been fabricated by pressureless sintering of compacts of attrition milled powder mixtures. Successful fabrication of high-strength and high toughness composites requires fine and homogeneous powders. Strength and fracture toughness of the composites increase with increasing milling time. Short milling times do not lead to the required particle fineness and powder homogeneity. For a composite containing 50 vol% Nb, strengths of up to 690 MPa with corresponding fracture toughness of 6·6 ± 0·4 MPa $m^{1/2}$ and hardness of 11·2 GPa (H_{V20}) have been obtained, whereas strengths of 592 MPa, fracture toughness of 6·6 ± 0·3 MPa $m^{1/2}$ and hardness of 9·3 GPa have been obtained for Cr–Al_2O_3 composites. © *1998 Elsevier Science Limited. All rights reserved*

1 Introduction

The primary mechanism responsible for increased toughness of metal-containing ceramics is the plastic bridging of metal ligaments causing crack closure forces which shield the crack tip.[1–4] Metal-reinforced Al_2O_3 has attractive mechanical properties especially when designed with interpenetrating networks.[5–7]

In the present work, the pressureless sintering of Nb–Al_2O_3 and Cr–Al_2O_3 composites has been studied; Nb and Cr were chosen because of their refractory character (T_m = 2468°C and 1875°C, respectively), similar linear thermal expansion coefficients ($\alpha_{Nb} = 7{\cdot}1\ 10^{-6}\ K^{-1}$ and $\alpha_{Cr} = 6\ 10^{-6}\ K^{-1}$) to Al_2O_3, and because of the ability of Nb and Cr to form a strong bond with Al_2O_3[8–11] and the stability of Nb/Al_2O_3 and Cr/Al_2O_3 interfaces during heat treatment at relatively high temperatures.[12–16]

*To whom correspondence should be addressed.

Pressureless sintered Nb/Al_2O_3 composites exhibited outstanding preliminary results in terms of high strength and toughness, as reported recently.[17] The high-temperature strength, thermal-shock resistance, and oxidation resistance reported in the past for Cr/Al_2O_3 cermets[18,19] with interpenetrating networks make these materials specially interesting for high temperature applications and worthy for revisit.

The microstructural development and mechanical properties of pressureless sintered Nb–Al_2O_3 and Cr–Al_2O_3 composites containing 50 vol% metal are reported. The principles of the fabrication method used and important processing parameters controlling microstructure and mechanical properties, such as milling intensity, sintering temperature, and sintering time are discussed.

2 Experimental Procedure

Powder mixtures containing Al_2O_3 (Ceralox HPA-0·5, Condea Chemie GmbH, Brunsbuettel, Germany, median particle size: 0·3 μm, D_{90}: 0·5 μm) and 50 vol% Nb (H. C. Starck GmbH, Goslar, Germany, median particle size: 6 μm, D_{90}: 10·1 μm) or 50 vol% Cr (Alfa, Johnson Matthey GmbH, Kalsruhe, Germany, median particle size: 13·2 μm, D_{90}: 42 μm) were attrition milled in acetone with 3-mm-diameter 3Y-TZP balls at 700 rpm. The 500-ml Al_2O_3-lined attrition mill (Netzsch PE 075, Netzsch-Feinmahltechnik, Germany), fitted with 3Y-TZP stirrer arms was filled with 5 vol% powder, 40 vol% liquid, and 50 vol% balls. Milling intensity was varied by changing the milling time (1, 3.5, and 7 h). Samples were designed for convenience M–Al_2O_3–xh, were M represents Nb or Cr and x the milling time. After milling, the precursor powders were dried and passed through a 200 μm sieve. The particle size of as-received and as-milled powders was determined using a Master Sizer S (Malvern Instruments Ltd., Malvern, UK)

with a reverse Fourier optic unit after 90s ultrasonic treatment in ethanol. Green samples were uniaxially pressed at 50 MPa into 5×4× 40 mm bodies followed by cold isostatical pressing at 900 MPa. Samples were heat treated in vacuum ($\sim 10^{-3}$ bar) in a graphite-heated furnace equipped with a dilatometer. Constant heating rate of 30°C min^{-1} between room and sintering temperature has been used for Nb–Al_2O_3 compacts. In order to obtain high densities, Cr–Al_2O_3 samples were heated using constant heating rate of 3°C min^{-1} from room temperature to 900°C and 30°C min^{-1} from 900°C to sintering temperature. Higher heating rates caused a large amount of residual porosity within the sintered samples. The relation between the heating rate used between room temperature and 900°C and the final density has not been clarified yet. Sintering was carried out at temperatures between 1450° and 1550°C, followed by a sintering hold of 1 to 3 h. X-ray diffraction analysis (XRD) obtained with powdered specimens was used to qualitatively determine the phase composition before and after thermal treatments.

Microstructural development was examined by scanning electron microscopy (SEM) and conventional transmission electron microscopy (TEM). Green densities were estimated from mass and volume of the compacts using theoretical densities of the individual components, whereas bulk densities of the sintered specimens were determined in water using Archimedes' principle. Hardness was measured at room temperature using a diamond Vickers indenter with a loading time of 10 s at a constant load of 200 N. The results were averaged over five indentations per specimen. Fracture strength and ISB-fracture toughness[20] were determined in four-point bending (span 10/20 mm) at 1 mm min^{-1} cross head speed using six samples ground and polished to 3 μm finish on the tensile surface. Fracture always occurred within 20 s. Crack-path observations were performed using cracks originating from Vickers indents.

3 Results and Discussion

Nb–Al_2O_3 powders attrition milled during 1 and 3·5 h still show the starting bimodal particle size distribution. The first mode of the distribution located at ~0·3 μm, which corresponds to the median particle size of Al_2O_3, and the second mode located at ~6 μm which corresponds to the median particle size of Nb. Increasing milling time results in further reduction of the particle size and a monomodal particle size distribution. After 7 h milling, the precursor Nb–Al_2O_3 powder has a median particle size < 3 μm. Cr–Al_2O_3 powders attrition milled during 1 h show a monomodal particle size distribution with a median particle size of 13 μm indicating that during low intensity milling median particle size remain almost constant, and that Al_2O_3 and Cr particles are rapidly brought together or adhered during milling. During different milling stages, only Nb or Cr and Al_2O_3 were observed using XRD.

The dilatometer curve of Nb–Al_2O_3 and Cr–Al_2O_3 compacts show that most of the shrinkage takes place above 850°C. Overall linear shrinkage of the samples Nb–Al_2O_3–7 h is ~12% whereas Cr–Al_2O_3–7 h is ~15%. For compositions studied, sintering temperatures > 1550°C for Nb–Al_2O_3 samples, > 1500°C for Cr–Al_2O_3 samples and sintering for more than 1 h did not significantly increase the final density. Sintered Nb–Al_2O_3 composites are composed of Nb and Al_2O_3 with traces of NbO, whereas Al_2O_3 peaks in sintered Cr–Al_2O_3 composites are shifted to low angles indicating that Cr ions had diffused into Al_2O_3 lattice. No compound or oxide of Cr could be identified. Therefore only Cr–Al_2O_3 solid solution and Cr could be identified. The high electrical conductivity of Nb–Al_2O_3 and Cr–Al_2O_3 composites, obtained using a two contact method in air, shows formation of a metal network.

Green density, relative densities after sintering, bending strengths, fracture toughnesses, and mean values of hardness as function of milling intensity are given in Table 1(a) and (b). The relatively high green densities when compared to pure Al_2O_3 (55 ± 1%TD) are due to the plastic deformation of metal particles during compaction resulting in strong metal/metal contacts leading to high green strengths. Green density decrease with increasing milling intensity whereas milling time > 3·5 h did not increase sintered final density, bend strength, toughnesses and hardness. Although high milling intensity assists the comminution of metal particles, extended milling does not benefit the mechanical properties. SEM photographs of polished sintered metal-Al_2O_3 composites showing the microstructure obtained using different milling intensity are presented in Figs 1 and 2. Microstructures fabricated from powder mixtures milled ≥3·5 h are quite dense with little porosity or defects visible. It is interesting to note that, the original flakelike shapes of metal particles can be recognised in the final microstructures in samples containing Cr even in Cr–Al_2O_3–7 h, whereas Nb flakes present in microstructure Nb–Al_2O_3–1 h disappear completely in Nb–Al_2O_3–7 h. The high values of fracture toughness determined, composites are nearly twice as tough as Al_2O_3, could be related to crack deflection and crack bridging. A crack induced by a Vickers indentor in a Nb–Al_2O_3

Table 1. Green density, relative density after sintering, bending strength, fracture toughness and mean hardness value of (a) Nb–Al_2O_3 and (b) Cr–Al_2O_3 composites

Designation	*Milling time (h)*	*Green density (% TD)*	*Density after sintering (% TD)*	*Bending strength (MPa)*	*Fracture toughness ($MPa m^{1/2}$)*	*Hardness (H_v 20) (GPa)*
(a)						
50Nb–1 h	1	68	79	254 ± 22	2·6 ± 0·2	7·6
50Nb–3·5 h	3·5	66·6	96·4	694 ± 62	6·6 ± 0·4	11.2
50Nb–7 h	7	63	96·7	674 ± 55	6·3 ± 0·3	11·8
(b)						
50Cr–1 h	1	66·1	94·1	384 ± 25	6·8 ± 0·3	6·7
50Cr–3·5 h	3·5	65	96·4	592 ± 51	6·6 ± 0·3	9.3
50Cr–7 h	7	62·9	96·4	570 ± 47	6·8 ± 0·4	9·3

and Cr–Al_2O_3 sample is shown in Fig. 3(a) and (b). Fracture surface observations show metal particles which have been plastically deformed and stretched to failure by necking accompanied of partial debonding at the interface metal/Al_2O_3. In both composites most Al_2O_3 grains are about 1 μm, i.e. Al_2O_3 grains don't grow much during sintering. Nevertheless, fracture surface of Nb–Al_2O_3–3·5 h show some Al_2O_3 grains > 5 μm. Such anomalous Al_2O_3 grain growth was not observed in Nb–Al_2O_3–

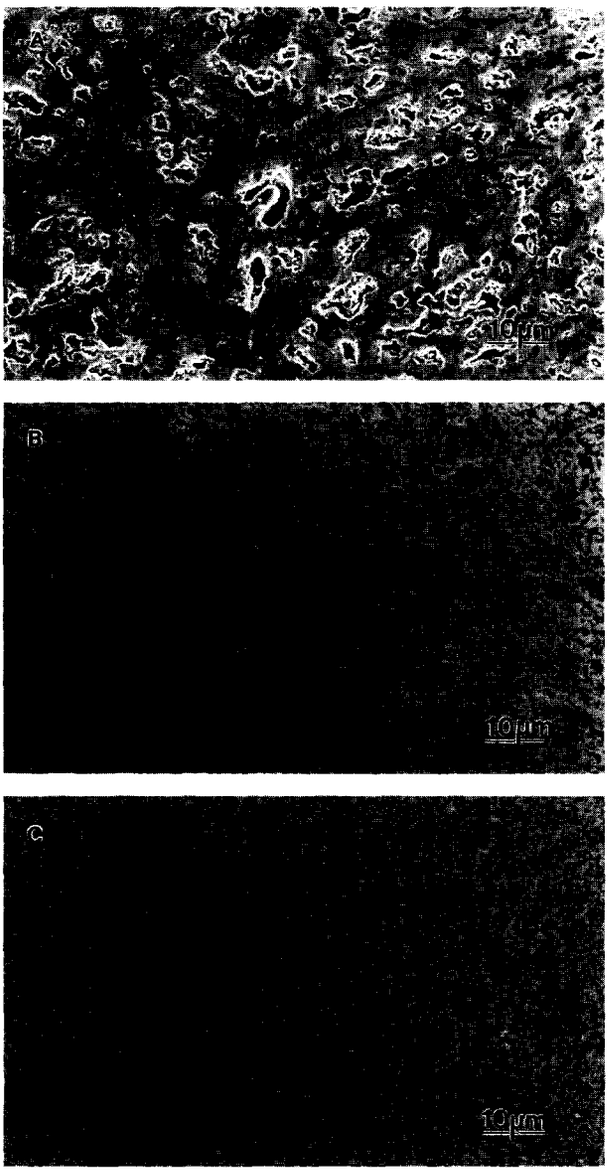

Fig. 1. SEM micrographs of polished microstructures of Nb/Al_2O_3 composites sintered 1 h at 1550°C fabricated from powder mixtures milled for (a) 1 h, (b) 3·5 h, and (c) 7 h.

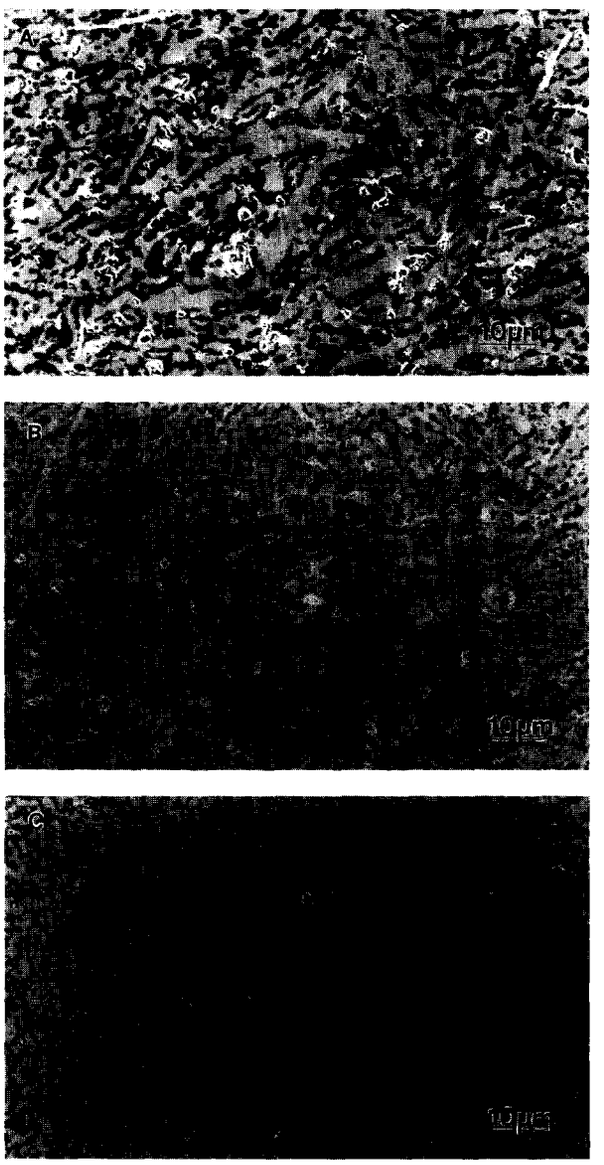

Fig. 2. SEM micrographs of polished microstructures of Cr/Al_2O_3 composites sintered 1 h at 1500°C fabricated from powder mixtures milled for (a) 1 h, (b) 3·5 h, and (c) 7 h.

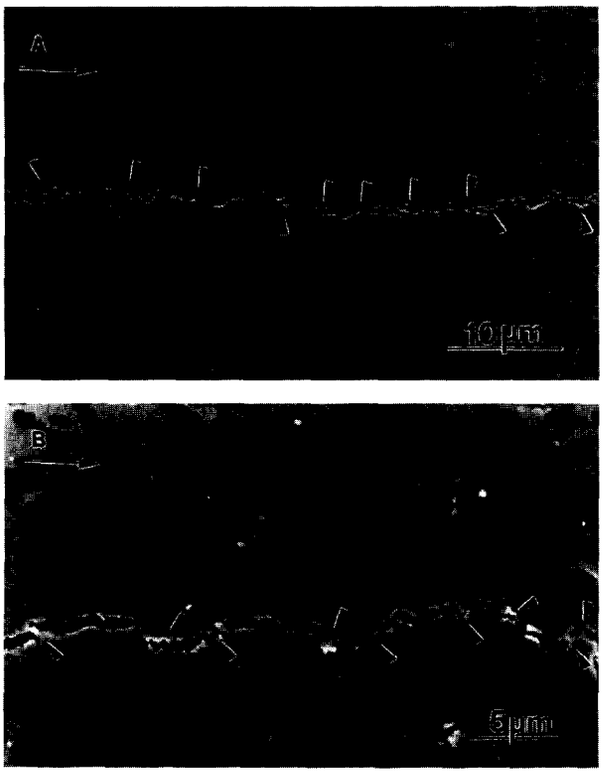

Fig. 3. SEM micrograph of crack propagation from Vickers indent ($P = 100$ N) in (a) Nb–Al_2O_3–3·5 h composite sintered 1 h at 1550°C, and (b) Cr–Al_2O_3–3·5 h composite sintered 1 h at 1500°C Arrows indicate crack bridging and crack propagation direction.

7 h. It is thought that increasing milling intensity, the resulting monomodal particle size distribution created restricting the number of Al_2O_3 grains that are in contact with each other which further limits exaggerated grain growth. The TEM observations indicates that Nb/Al_2O_3 and Cr/Al_2O_3 interfaces are well-bonded. No interfacial cracks are observed indicating a low residual stress level.

4 Conclusions

1. Dense (> 96% TD) Al_2O3-matrix composites containing 50 vol% of Nb or 50 vol% of Cr can be fabricated by intensive attrition milling followed by pressureless sintering.
2. Milling intensity is the decisive factor order to obtain dense metal–Al_2O_3 composites and high mechanical properties.
3. Strong interfacial bonding of the composite and possibly similar thermal expansion coefficients of Nb, Cr and Al_2O_3 are responsible for a toughness twice that of Al_2O_3 and high values of bending strengths.
4. The high fracture toughness (> 6·3 MPa $m^{1/2}$) of Nb–Al_2O_3 and Cr–Al_2O_3 composites can be attributed to different toughening mechanisms including crack deflection and in some extension crack bridging by the ductile metal ligaments.

Acknowledgements

Financial support by the German Research Foundation (DFG) under contract No. Ja 655/4 and helpful technical assistance of Axel Krupp are gratefully acknowledged.

References

1. Krstic, J. T., On the fracture of brittle-matrix/ductile-particle composites. *Philos. Mag.*, 1983, **A 48**(5), 695–708.
2. Sigl, L. S., Mataga, P. A., Dalgleish, B. J., McMeeking, R. M. and Evans, A. G., On the toughness of brittle materials reinforced with a ductile phase. *Acta Metall.*, 1988, **36**(4), 945–953.
3. Ashby, M. F., Blunt, F. J. and Bannister, M., Flow characteristics of highly constrained metal wires. *Acta Metall.*, 1989, **37**(7), 847–1857.
4. Flinn, B. D., Ruehle, M. and Evans, A. G., Toughening in Composites of Al_2O_3 reinforced with Al. *Acta Metall.*, 1989, **37**(11), 3001.
5. Prielipp, H., Knechtel, M., Claussen, N., Streiffer, S. K., Muellejans, H., Ruehle, M. and Roedel, J., Strength and fracture toughness of aluminum/alumina composites with interpenetrating networks. *Mat. Sci. and Eng.*, 1995, **A 197**, 19–30.
6. Knechtel, M., Prielipp, H., Muellejans, H., Claussen, N. and Roedel, J., Mechanical properties of Al/Al_2O_3 and Cu/Al_2O_3 composites with interpenetrating networks. *Scr. Metall et Mater.*, 1994, **31**, 1085–1090.
7. Roedel, J., Prielipp, H., Claussen, N., Sternitzke, M., Alexander, K. B., Becher, P. F. and Schneibel, J. H., Ni_3Al/Al_2O_3 composites with interpenetrating networks. *Scr. Metall et Mater.*, 1995, **33**, 843–848.
8. Mader, W. and Ruehle, M., Electron microscopy studies of defects at diffusion-bonded Nb/Al_2O_3 interfaces. *Acta Metall.*, 1989, **37**(3), 853–866.
9. Bruley, J., Brydson, R., Muellejans, H., Mayer, J., Gutekunst, G., Mader, W., Knauss, D. and Ruehle, M., Investigation of the chemistry and bonding at niobium-sapphire interfaces. *J. Mater. Res.*, 1994, **9**(10), 2574.
10. Ruehle, M., Structure and composition of metal/ceramic interfaces. *J. Eur. Ceram. Soc.*, 1996, **16**, 353–365.
11. Blackburn, A. R., Shevlin, T. S. and Lowers, H. R., Fundamental study and equipment for sintering and testing of cermet bodies: I-III. *J. Am. Ceram. Soc.*, 1949, **32**(3), 81–98.
12. Economos, G. and Kingery, W. D., Metal-ceramic interactions: II, metal-oxide interfacial reactions at elevated temperatures. *J. Am. Ceram. Soc.*, 1953, **36**(12), 403–409.
13. Economos, G., Behavior of refractory oxides in contact with metals at high temperatures. *J. Metals*, 1953, **45**, 458–459.
14. Tressler, R. E., Interfaces in oxide reinforced metals. In *Interfaces in Metal Matrix Composites*, Vol. 1, ed. G. Metcalfe. Academic Press, London, 1974.
15. Shaw, L., Miracle, D. and Abbaschian, R., Microstructure and mechanical properties of metal/oxide and metal/silicide interfaces. *Acta Metall. Mater.*, 1995, **12**, 4267.
16. Shevlin, T. S. Oxide-base cermets, and Marshall, C. L. Chromium-alumina base cermets, In *Cermets*, ed. J. R. Tinklepaugh and W. B. Crandall. Reinhold Publishing Corp, New York, 1960, pp. 97–109, 109–118.

17. García, D. E., Schicker, S., Bruhn, J., Janssen R. and Claussen, N. Processing and mechanical properties of pressureless sintered Nb–Al_2O_3 matrix composites. *J. Am. Ceram Soc.*, in press.
18. Blackburn, A. R. and Shevlin, T. S., Fundamental study and equipment for sintering and testing of cermet bodies: V, fabrication, testing, and properties of 30 chromium-70 alumina cermets. *J. Am. Ceram. Soc.*, 1951, **34**(11), 327–331.
19. Shevlin, T. S., Fundamental study and equipment for sintering and testing of cermet bodies: VI, fabrication, testing, and properties of 72 chromium-28 alumina cermets. *J. Am. Ceram. Soc.*, 1954, **37**(3), 140–145.
20. Chantikul, P., Anstis, G. R., Lawn, B. R. and Marshall, D. B., A critical evaluation of indentation techniques for measuring fracture toughness: II, strength method. *J. Am. Ceram. Soc.*, 1981, **64**(9), 539–543.